ELSEVIER

Inorganica Chimica Acta 225 (1994) 15–22

Inorganica Chimica Acta

Predicting the effect of oxidative doping on the conductivities of metal–tetrakis(dimethylphosphino)benzene coordination polymers from the electrochemical properties of their related bimetallic complexes

Pei-Wei Wang, Marye Anne Fox*

Department of Chemistry and Biochemistry, University of Texas, Austin, TX 78712, USA

Received 8 February 1994

Abstract

Intermetallic electronic coupling in 1,2,4,5-tetrakis(dimethylphosphino)benzene bridged bimetallic Ni, Pd and Pt complexes has been studied by electrochemical and spectroelectrochemical methods. These bimetallic complexes show minimal cross-ring metal–metal interactions. The observed oxidation potential for the monometallic Ni^{II} complex is similar to that of its bimolecular analog, but substantial shifts from the monometallic complexes are observed for the Pd^{II} and Pt^{II} complexes. The very low conductivities observed in the metal–phosphine coordination polymers ($M = Ni^{II}$, Pd^{II}, Pt^{II}) and their partially-oxidized (p-doped) analogs are consistent with the minimal coupling observed in the bimetallic complexes.

Keywords: Nickel complexes; Palladium complexes; Platinum complexes; Coordination polymer complexes

1. Introduction

A variety of metal coordination polymers incorporating square planar metal centers and conjugated bridging ligands exhibit enhanced electrical conductivity. These include metal coordination polymers of tetrathiooxalate [1–4], dihydroxybenzoquinone [5] and tetraaminobenzene [6]. Preparation of a conductive coordination polymer requires (i) redox-active metal centers arranged to permit strong metal–metal interaction, which often entails close spatial proximity and similar crystallographic and electronic environments for the metals; and (ii) partial oxidation or reduction to a stable mixed-valence state to facilitate charge transfer along the macromolecular backbone.

Enhanced conductivity in metal–phosphine coordination polymers ($M = Ni^{II}$, Pd^{II}, Pt^{II}) can be reasonably expected because the polymers contain several key structural features favoring conductivity [7–9]: (i) different stable oxidation states of the metal–phosphine complex offer the possibility of creating a mixed-valence polymer backbone; (ii) the square planar geometries of Ni^{II}, Pd^{II} and Pt^{II} phosphine complexes allow for strong metal–metal interactions in a rigid, flat polymer backbone. Previously, we have observed increased intermetallic electronic coupling in several reduced mixed-valence Ni^{I}–Ni^{0}, Pd^{II}–Pd^{0} and Pt^{II}–Pt^{0} complexes [10]. However, the metal–metal interactions in these reduced mixed-valence (n-doped) coordination polymers were adversely affected by an accompanying geometry change at the reduced metal center. To obviate this problem, the conductivities of the analogously oxidatively doped metal–phosphine coordination polymers were examined.

In this paper, we describe the preparation of metal–tmpb (tmpb = 1,2,4,5-tetrakis(dimethylphosphino)benzene) coordination polymers **1a**–**c**. The electrical conductivities of polymers **1a**–**c** and their partially-oxidized analogs were determined. Model bimetallic $[(L)MCl_2\text{–tmpb–}MCl_2(L)]$ (M = Ni [9], Pd or Pt; L = 1,2-bis(dimethylphosphino)benzene, dmpb or 1,2-bis(diisopropylphosphino)benzene, dippb) com-

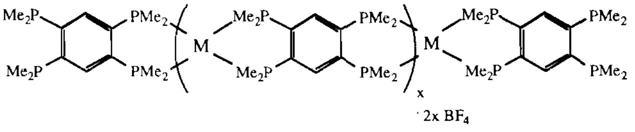

1a, $M = Ni^{II}$
1b, $M = Pd^{II}$
1c, $M = Pt^{II}$

---

*Corresponding author.

SSDI 0020-1693(94)04024-P

plexes **2a–c** were also prepared, and the intermetallic electronic couplings in the model complexes were investigated by electrochemical and spectroelectrochemical methods. The results are discussed in relation to the observed conductivity of the polymers **1a–c** and their corresponding Cl_2-doped polymer films.

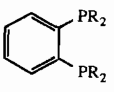

dmpb, R = Me

dippb, R = ^iPr

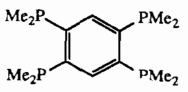

tmpb

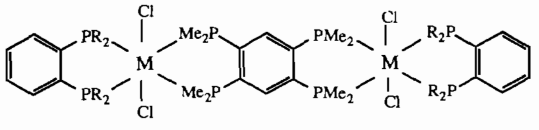

2a, M = Ni^{II}; R = Me

2b, M = Pd^{II}; R = ^iPr

2c, M = Pt^{II}; R = ^iPr

2d, M = Pd^{IV}; R = ^iPr

2e, M = Pt^{IV}; R = ^iPr

2. Experimental

2.1. Physical measurements

Electrochemical measurements were carried out with a Princeton Applied Research model 173 potentiostat equipped with a model 179 digital coulometer and a model 175 universal programmer of a BAS 100 electrochemical analyzer. Typical experiments were run at 100 mV/s in CH_3CN with 0.1 M tetrabutylammonium hexafluorophosphate. For cyclic voltammetry, a Ag/AgCl wire was used as a quasi-reference electrode, a Pt wire as the counter electrode, and a Pt disk as the working electrode. Ferrocene was used as an internal standard to calibrate the observed potential (versus SCE) [11]. For bulk electrolysis, a Pt flag was used as the working electrode, SCE as the reference electrode, and a carbon cloth as the counter electrode.

Proton-decoupled ^{31}P NMR spectra were measured on a Nicolet NT-360 spectrophotometer, referenced to 85% H_3PO_4 in D_2O. ^1H NMR spectra were measured on a General Electronic QE300 spectrophotometer. Chemical shifts were reported in ppm from a tetramethylsilane or a H_3PO_4 reference. Conductivity measurements were made by a previously described two-probe technique on a pressed powder sample in a sandwich cell with a thickness of ~1 mm. Absorption spectra were measured on a Hewlett-Packard 8451A diode array spectrophotometer. Elemental analyses were obtained from the Galbraith Laboratories. Profilometry was measured on a Tencor Instruments alpha-step 100.

2.2. Materials

1,2-Bis(diisopropylphosphino)benzene (dippb) [12], 1,2,4,5-tetrakis(dimethylphosphino)benzene (tmpb) [9], $[Ni(CH_3CN)_6](BF_4)_2\cdot\frac{1}{2}(CH_3CN)$ [13], $[Pd(CH_3CN)_4](BF_4)_2$ [14], (dippb)$PdCl_2$ [15] and (dippb)$PtCl_2$ [15] were prepared by literature methods. 1,5-Cyclooctadiene platinum chloride ((COD)$PtCl_2$) was used as received from Aldrich.

*2.2.1. Poly-[Ni-1,2,4,5-tetrakis(dimethylphosphino)benzene]$_{48}$(BF_4)$_{96}$ (**1a**)*

A solution of tmpb (101 mg, 0.32 mmol) in 10 ml of CH_2Cl_2 was added to a solution of $[Ni(CH_3CN)_6](BF_4)_2\cdot\frac{1}{2}(CH_3CN)$ (158 mg, 0.32 mmol) in 5 ml of CH_3CN under Ar. The resulting solution was stirred for 24 h at room temperature. The solid product was collected by Schlenk filtration, washed with CH_2Cl_2 (25 ml), CH_3CN (10 ml), and vacuum dried. Yield 170 mg (98%). *Anal.* Calc. for $(C_{14}H_{26}P_4NiB_2F_8)_{48}$: C, 30.54; H, 4.76. Found: C, 28.31; H, 5.02%.

End-group analysis was performed by stirring a suspension of the polymer with excess tmpb in CH_2Cl_2 to cap each metal-terminated polymer chain. After the resulting mixture had been stirred for 24 h at r.t. under Ar, the solid product was collected by Schlenk filtration, washed with CH_2Cl_2, and vacuum dried. The average number of repeat units can be calculated from the ratio of the integrated peak areas assigned to coordinated to non-coordinated phosphines in the resulting tmpb end-capped polymer. **1a**, $M=Ni^{II}$: ^{31}P NMR (1/3 of $CDCl_3$/DMF): δ 43 (coordinated), −48 (non-coordinated). The integration ratio of coordinated to non-coordinated phosphines is 48 ± 7, from which the molecular weight is calculated as 26 000 ± 4000.

*2.2.2. Poly-[Pd-1,2,4,5-tetrakis(dimethylphosphino)benzene]$_{80}$(BF_4)$_{160}$ (**1b**)*

A solution of tmpb (193 mg, 0.61 mmol) in 40 ml of CH_2Cl_2 was added to a solution of $[Pd(CH_3CN)_4](BF_4)_2$ (270 mg, 0.61 mmol) in 40 ml of CH_3CN under Ar. The resulting solution was stirred for 24 h at r.t. The solid product was collected by Schlenk filtration, washed with CH_3CN (50 ml), CH_2Cl_2 (25 ml), and vacuum dried. Yield 340 mg (93%). *Anal.* Calc. for $(C_{14}H_{26}P_4PdB_2F_8)_{80}$: C, 28.11; H, 4.38. Found: C, 26.67; H, 4.88%.

End-group analysis as described for **1a**. **1b**, $M=Pd^{II}$: ^{31}P NMR (1/3 of $CDCl_3$/DMF): δ 40 (coordinated), −48 (non-coordinated). The integration ratio of coordinated to non-coordinated phosphines is 80 ± 10. The molecular weight is therefore calculated as 48 000 ± 6000.

2.2.3. Poly-[Pt-1,2,4,5-tetrakis(dimethylphosphino)-benzene]$_{28}$(BF$_4$)$_{56}$ (1c)

Tetrafluoroboric acid (0.1 ml of an 85% solution in ether) was added via syringe to a solution of (COD)PtCl$_2$ (56 mg, 0.15 mmol) in 15 ml of CH_2Cl_2. After the resulting solution had been stirred for 5 min, a solution of tmpb (48 mg, 0.15 mmol) in 15 ml of CH_2Cl_2 was added under Ar. After the resulting solution was stirred for 24 h at r.t. under Ar, the solid product was collected by Schlenk filtration, washed with 25 ml of CH_2Cl_2, and vacuum dried. Yield 100 mg (97%). *Anal.* Calc. for $(C_{14}H_{26}P_4PtB_2F_8)_{28}$: C, 24.48; H, 3.82. Found: C, 23.65; H, 3.09%.

End-group analysis was performed as with **1a**. **1c**, M = Pt^{II}: ^{31}P NMR (1/3 of CDCl$_3$/DMF): δ 33 (coordinated, $^1J(^{195}Pt–P) = 2320$ Hz), −49 (non-coordinated). The integration ratio of coordinated to non-coordinated phosphines is 28±5. The molecular weight is therefore calculated as 19 000±3000.

2.2.4. [1,2-Bis(diisopropylphosphino)benzene]-MCl$_2$-(1,2,4,5-tetrakis(dimethylphosphino)benzene)-MCl$_2$-[1,2-bis(diisopropylphosphino)benzene], [(dippb)MCl$_2$-tmpb-MCl$_2$(dippb)] (2b,c)

A solution of tmpb (0.19 mmol) in 15 ml of CH_2Cl_2 was transferred under Ar to a solution of (dippb)MCl$_2$ (M = Pd or Pt) (0.38 mmol) in 15 ml of CH_2Cl_2. The resulting mixture was stirred for 5 min before the solution was concentrated to ~5 ml under reduced pressure. The solid product was collected by filtration and recrystallized from CH_3CN/ether.

2b, M = Pd^{II}: yield 83%. ^{31}P NMR (CD$_3$CN): δ 78.5 (d, J(PP) = 312 Hz, 4P), 33.1 (d, J(PP) = 312 Hz, 4P). ^{1}H NMR (CD$_3$CN): δ 9.49 (m, 2H), 7.92 (m, 4H), 7.76 (m, 4H), 2.85 (m, 8H), 2.43 (d, J = 10 Hz, 24H), 1.37 (dd, J = 14 and 7 Hz, 24H), 1.20 (dd, J = 19 and 7 Hz, 24H). *Anal.* Calc. for $C_{50}H_{90}P_8Pd_2Cl_4$: C, 46.42; H, 7.01. Found: C, 44.90; H, 6.76%.

2c, M = Pt^{II}: yield 99%. ^{31}P NMR (CD$_3$NO$_2$): δ 70.4 (td, J(PP) = 280 Hz, $^1J(^{195}Pt–P) = 2288$ Hz, 4P), 30.1 (td, J(PP) = 280 Hz, $^1J(^{195}Pt–P) = 2288$ Hz, 4P). ^{1}H NMR (CD$_3$CN): δ 9.37 (m, 2H), 8.27 (m, 4H), 7.96 (m, 4H), 3.24 (m, 8H), 2.64 (d, J = 11 Hz, 24H), 1.54 (dd, J = 14 and 6 Hz, 24H), 1.32 (dd, J = 19 and 6 Hz, 24H). *Anal.* Calc. for $C_{50}H_{90}P_8Pt_2Cl_4$: C, 40.83; H, 6.17. Found: C, 38.90; H, 5.92%.

2.2.5. [1,2-Bis(diisopropylphosphino)benzene]-MCl$_2$-(1,2,4,5-tetrakis(dimethylphosphino)benzene)-MCl$_2$-[1,2-bis(diisopropylphosphino)benzene] chloride, [(dippb)MCl$_2$-tmpb-MCl$_2$(dippb)]·4Cl (2d,e)[1]

Cl$_2$ (0.30 mmol, excess) in 1 ml of CCl$_4$ was added to a suspension of **2b** or **2c** (0.03 mmol) in 5 ml of CCl$_4$. The resulting mixture was stirred 1 h. The solid was collected by filtration and was washed by CCl$_4$.

2d, M = Pd^{IV}: ^{31}P NMR (D$_2$SO$_4$/external H$_3$PO$_4$ in D$_2$O): δ 85.3 (d, J(PP) = 294 Hz, 4P), 31.7 (d, J(PP) = 294 Hz, 4P).

2e, M = Pt^{IV}. ^{31}P NMR (D$_2$SO$_4$/external H$_3$PO$_4$ in D$_2$O): δ 60.9 (td, J(PP) = 405 Hz, $^1J(^{195}Pt–P) = 1400$ Hz, 4P), 24.8 (td, J(PP) = 405 Hz, $^1J(^{195}Pt–P) = 1400$ Hz, 4P).

2.3. Conductivity measurements of Cl$_2$-doped polymers 1a–c

A thin film (~1.5 μm, determined by profilometry) of **1a–c** was obtained by casting the polymer solution (5 μl of a 0.6 mM DMSO solution) on a gold sputtered two-probe electrode (with a thickness of ~1000 Å and a separation between two probes of ~ 2 mm) or microscopic slide. The polymer-film coated electrodes and slides were mounted in a Pyrex cuvette to which a bulb containing Cl$_2$ was attached. The conductivity change and the degree of oxidation of the polymer films **1a–c** were measured in situ on the gold electrode (conductivity) and microslide (absorption differences) during the reaction.

3. Results and discussion

3.1. Model complexes

The 1,2,4,5-tetrakis(dimethylphosphino)benzene-bridged bimetallic complexes **2a–c** were prepared by reacting 2 equiv. of (L)MCl$_2$ (L = dmpb, M = Ni^{II}; L = dippb, M = Pd^{II} or Pt^{II}) with 1 equiv. of tmpb. The electrochemical and spectroelectrochemical properties of the corresponding monometallic complexes **3a–c** have been reported by Warren and Bennett [16]. The monometallic complexes **3a–c** exist as the five-coordinate cations [(dmpb)$_2$MCl]·Cl with pseudo-square pyramidal geometry in solution [16]. The corresponding Ni^{III} or M^{IV} complexes (M = Ni, Pd or Pt) exhibit slightly tetragonally distorted octahedral geometries [17–19].

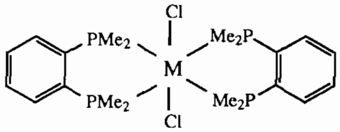

3a, M = Ni^{II}
3b, M = Pd^{II}
3c, M = Pt^{II}

Table 1 summarizes the oxidative peak potentials of **2a–c** and **3a–c** observed by cyclic voltammetry. The single redox wave (Ni$^{III/IV}$–Ni$^{III/IV}$) in the cyclic voltammogram of **2a** indicates that the presence of the

---

[1] The elemental analyses were not obtained due to the thermal instabilities of complexes.

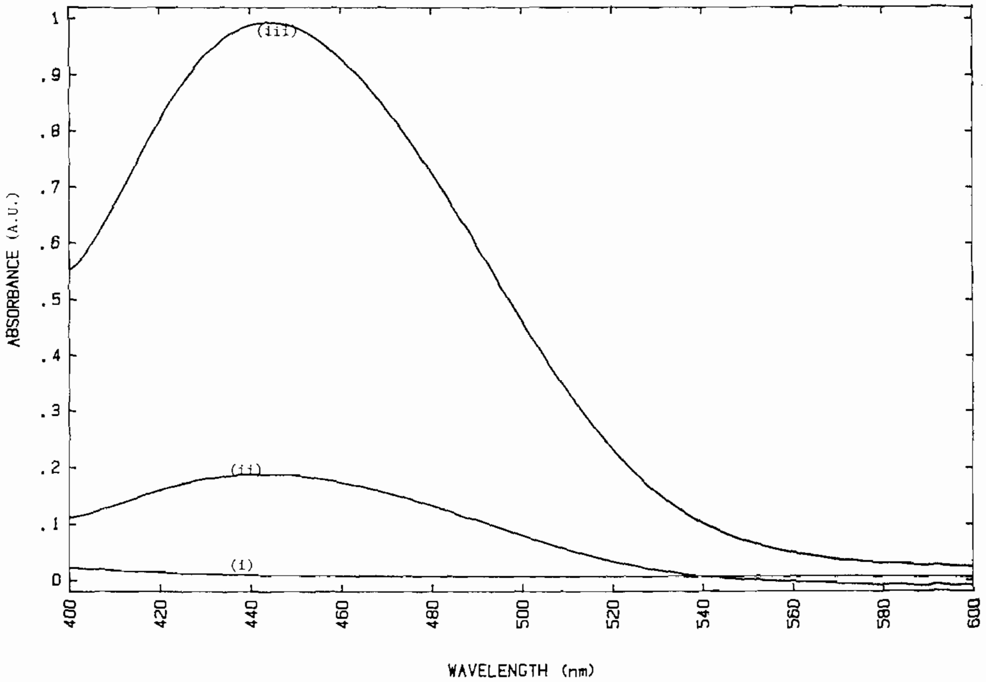

Fig. 1. Absorption spectra of: (i) bimetallic Pd^{II}–Pd^{II} complex **2b** in CH_3CN (1 mM); (ii) partially-oxidized Pd^{II}–Pd^{IV} complex in H_2SO_4 (1 mM); (iii) fully-oxidized Pd^{IV}–Pd^{IV} complex **2d** in H_2SO_4 (1 mM).

Table 1
Cyclic voltammetric peak potentials for the oxidation[a] of bimetallic complexes **2a–c** and monometallic complexes **3a–c**

Metal complex	Couple	*E* (V)
3a[b]	Ni^{III}/Ni^{IV}	0.69 (rev.)
2a[b]	Ni^{III}–Ni^{III}/Ni^{IV}–Ni^{IV}	0.71 (quasi-rev.)
3b[c]	Pd^{II}/Pd^{IV}	0.34 (irrev.)
2b	Pd^{II}–Pd^{II}/Pd^{IV}–Pd^{IV}	0.92 (irrev.)
3c[c]	Pt^{II}/Pt^{IV}	−0.04 (irrev.)
2c	Pt^{II}–Pt^{II}/Pt^{IV}–Pt^{IV}	0.95 (irrev.)

[a] Reaction conditions: scan rate, 100 mV/s; reference electrode, Ag/AgCl; counter electrode, Pt wire; working electrode, Pt disk; 0.1 M tetrabutylammonium hexafluorophosphate in CH_3CN under N_2 at room temperature.

[b] From Ref. [9].

[c] From Ref. [16].

second metal does not influence the redox chemistry of the first metal center. Furthermore, coulometry establishes that both metal centers are oxidized at the same potential, suggesting that there is little interaction between the nickel centers in the bimetallic complex. The observation of only single oxidation waves (4-electrons) in the bimetallic Pd^{II} and Pt^{II} complexes **2b,c** indicates that both of the metal centers are oxidized at the same potential. The redox potentials of the bimetallic complexes **2b,c** are significantly more positive than the monometallic complexes **3b,c** presumably because of the greater sterically induced distortion in the bimetallic Pd^{IV} by Pt^{IV} complexes **2d,e** than in the monometallic Pd^{IV} or Pt^{IV} complexes. Steric interactions with dippb and tmpb apparently destabilize the bimetallic Pd^{IV} or Pt^{IV} complexes **2d,e** relative to the interactions between two dmpb ligands in the monometallic Pd^{IV} or Pt^{IV} complex.

π-Backbonding interactions between M^{IV} and phosphine are weaker than in the M^{II}–phosphine complexes ($M = Pd$ or Pt) [20,21]. Therefore, the inaccessibility of stable mixed-valence Pd^{II}–Pd^{IV} and Pt^{II}–Pt^{IV} complexes in the electrochemical studies may contribute to the lack of intermetallic electronic coupling in the bimetallic complex. The partially oxidized bimetallic Pd^{II} and Pt^{II} complexes **2b,c** (produced by treatment with stoichiometric Cl_2 in CCl_4) do not exhibit detectable intervalence charge transfer (IT) bands, an observation that again indicates that the weakness or absence of intermetallic electronic coupling between two metal centers in the tmpb-bridged bimetallic complexes **2b,c** (Figs. 1 and 2).

The steric distortion of the bimetallic M^{IV} complexes **2d,e** can be further characterized by spectroelectrochemistry. The monometallic Pd^{IV} and Pt^{IV} complexes exhibit absorption spectra with $\lambda_{max} = 415$ and 313 nm, respectively [16]. These bands can be assigned to the d–d transition of the d^6 complexes in a tetragonally distorted octahedral geometry [19]. The Cl_2-oxidized bimetallic Pd^{IV}–Pd^{IV} and Pt^{IV}–Pt^{IV} complexes **2d,e** show red-shifted absorption spectra with $\lambda_{max} = 444$ ($\epsilon = 940$ M^{-1} cm^{-1}) and 350(sh) nm, respectively (Figs. 1 and 2). The red shift indicates a smaller energy gap between

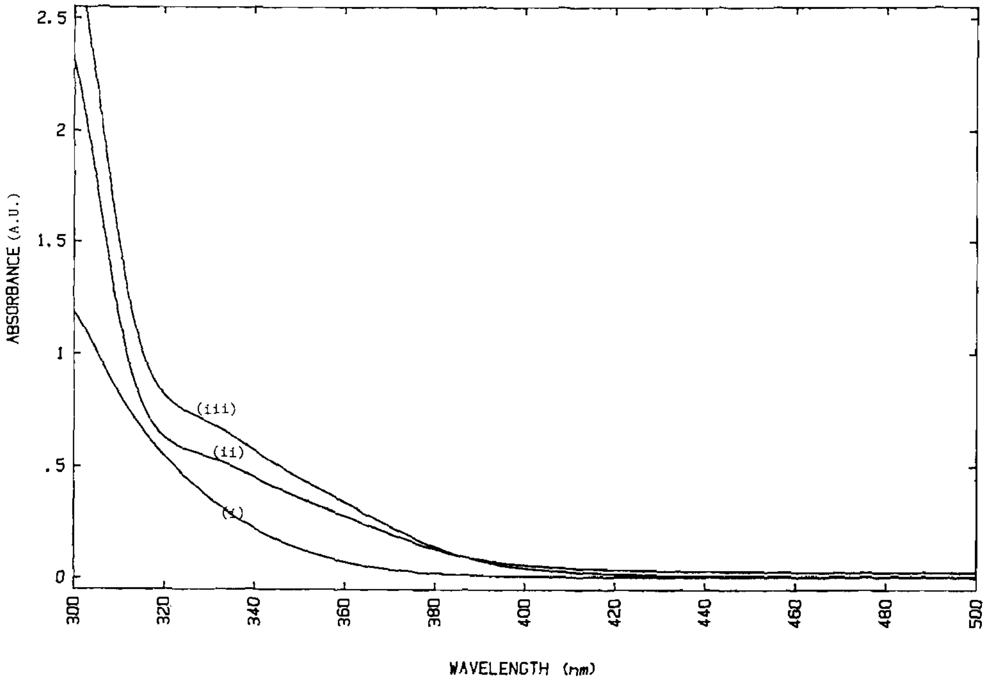

Fig. 2. Absorption spectra of: (i) bimetallic Pt^{II}–Pt^{II} complex **2c** in CH_3CN (0.1 mM); (ii) partially-oxidized Pt^{II}–Pt^{IV} complex in H_2SO_4 (0.1 mM); (iii) fully-oxidized Pt^{IV}–Pt^{IV} complex **2e** in H_2SO_4 (0.1 mM).

the non-bonding (HOMO) and antibonding (LUMO) orbitals in the bimetallic complexes **2d,e** than that of the corresponding monometallic M^{IV} complex. The energy of the antibonding orbital ($d_{x^2-y^2}$) in tetragonally distorted octahedral bimetallic complexes **2d,e** is lower than that of the corresponding monometallic M^{IV} complexes because of steric congestion in **2d,e** [22]. In contrast to the stabilization of the antibonding orbital ($d_{x^2-y^2}$, LUMO), steric distortion produces an enhanced antibonding interaction between the phosphine σ orbitals and metal non-bonding (d_{xz} and d_{yz}, HOMO) orbitals in the bimetallic Pd^{IV} or Pt^{IV} complex, which therefore destabilizes the filled non-bonding orbitals [22].

3.2. Metal-phosphine coordination polymers

Conductivities of the metal–phosphine coordination polymers **1a–c** measured as pressed powder samples in a sandwich cell with a two-probe technique are summarized in Table 2. The low conductivities of these coordination polymers indicate that the transition metals in the M^{II} oxidation states are only weakly coupled along the polymer backbone [23].

Table 2
Conductivities[a] of metal–phosphine coordination polymers **1a–c** and their partially-oxidized (p-doped) analogs

Compound	Conductivity (Ω^{-1} cm^{-1})[b]
1a ($M=Ni^{II}$)	$(7\pm3)\times10^{-9}$
1a (50% oxidation of metal centers)	$<10^{-9}$
1a (100% oxidation of metal centers)	$<10^{-9}$
1b ($M=Pd^{II}$)	$(7\pm2)\times10^{-8}$
1b (50% oxidation of metal centers)	$<10^{-8}$
1b (100% oxidation of metal centers)	$<10^{-8}$
1c ($M=Pt^{II}$)	$(8\pm5)\times10^{-8}$
1c (50% oxidation of metal centers)	$<10^{-8}$
1c (100% oxidation of metal centers)	$<10^{-8}$

[a] Conductivity was measured by the two-probe technique [9] on a pressed powder sample in a sandwich cell with a thickness of ~1 mm.

[b] Average of two measurements on independently prepared samples.

When the polymer films **1a–c** are treated by Cl_2 gas to effect a chemical oxidation, the extent of partial oxidation can be determined from changes in the absorption spectra of the partially-oxidized polymer films and their M^{II} analogs. The Ni^{II} polymer film **1a** exhibits an absorption spectrum with $\lambda_{max}=364$ nm, whereas the fully-oxidized Ni^{IV} polymer film displays an absorption spectrum with $\lambda_{max}=560$ nm (Fig. 3). The corresponding monometallic **3a** ($M=Ni^{II}$) and **3b** ($M=Ni^{IV}$) complexes show similar spectra with $\lambda_{max}=360$ and 565 nm, respectively [16]. The electronic spectrum of the Pd^{II} polymer film **1b** is similar to the corresponding monometallic Pd^{II} complex **3b** consisting of a metal–ligand charge transfer band at <300 nm. Both the fully-oxidized Pd^{IV} polymer film and monometallic Pd^{IV} complex show absorption spectra with

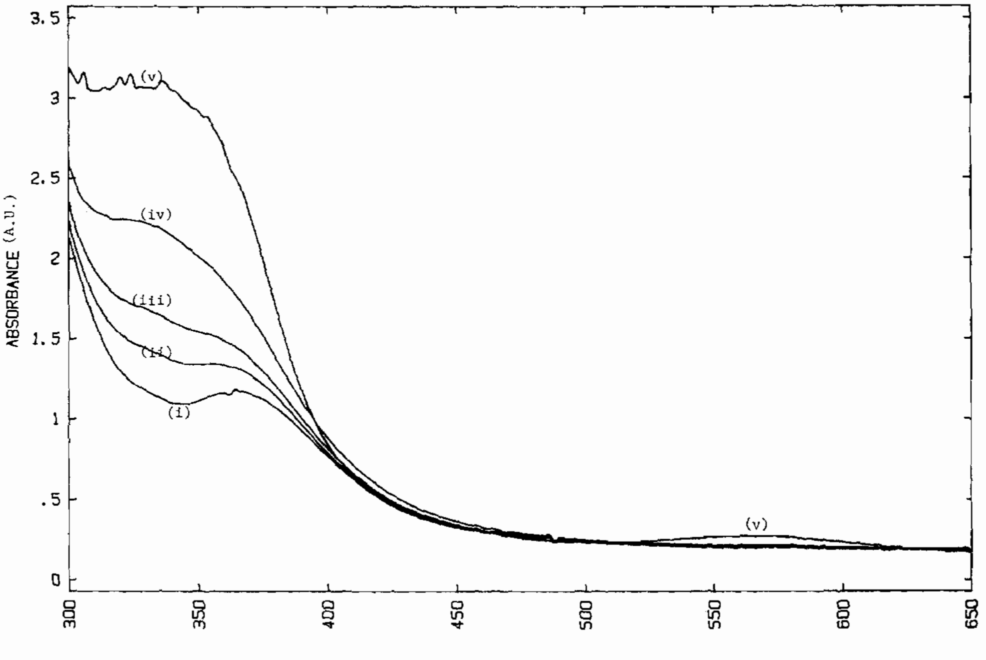

Fig. 3. Changes in absorption spectra of a thin film **1a** on a glass slide during oxidation by gaseous Cl_2: (i) **1a** (0% oxidation); (ii) 7% oxidation; (iii) 26% oxidation; (iv) 45% oxidation; (v) 100% oxidation. The degree of partial oxidation of the polymer films was determined by the relative absorption intensity at 364nm.

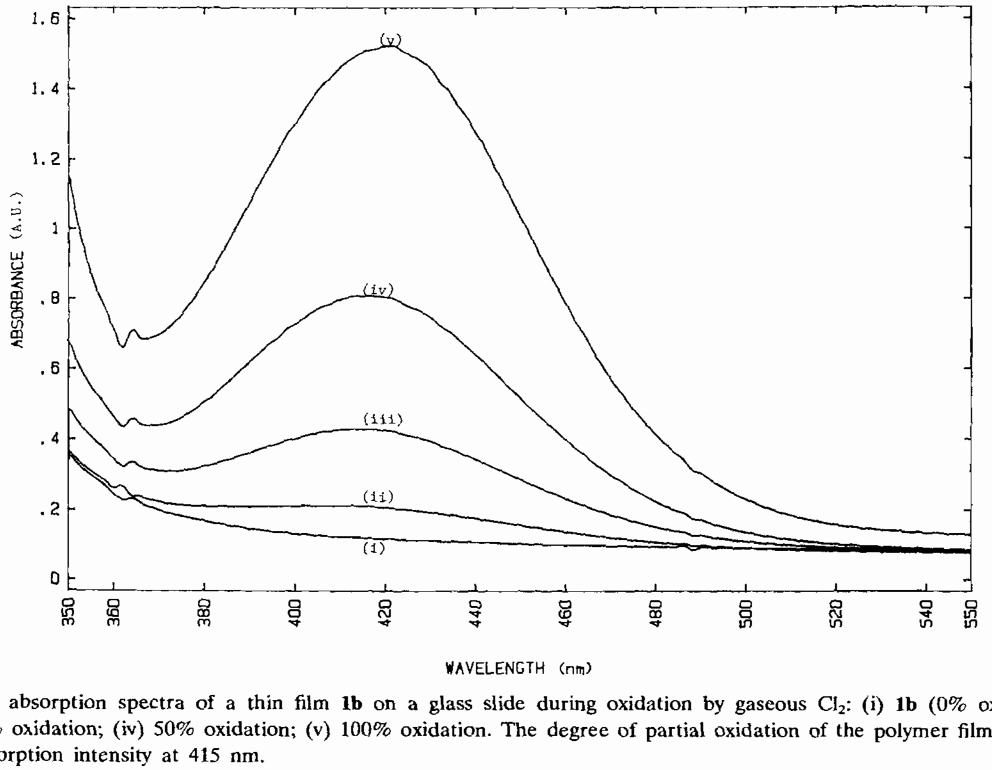

Fig. 4. Changes in absorption spectra of a thin film **1b** on a glass slide during oxidation by gaseous Cl_2: (i) **1b** (0% oxidation); (ii) 6% oxidation; (iii) 22% oxidation; (iv) 50% oxidation; (v) 100% oxidation. The degree of partial oxidation of the polymer films was determined by the relative absorption intensity at 415 nm.

λ_{max} =415 nm (Fig. 4) [16,19]. The Pt^{II} polymer film **1c** exhibits an absorption spectrum with λ_{max}=340 and 400(sh) nm, whereas the fully-oxidized Pt^{IV} polymer film shows an absorption spectrum with λ_{max}=313 nm (Fig. 5). The corresponding monometallic Pt^{IV} complex **3c** exhibits an identical spectrum [16].

The conductivities of the partially-oxidized polymer films **1a–c** during the Cl_2-doping reaction were followed

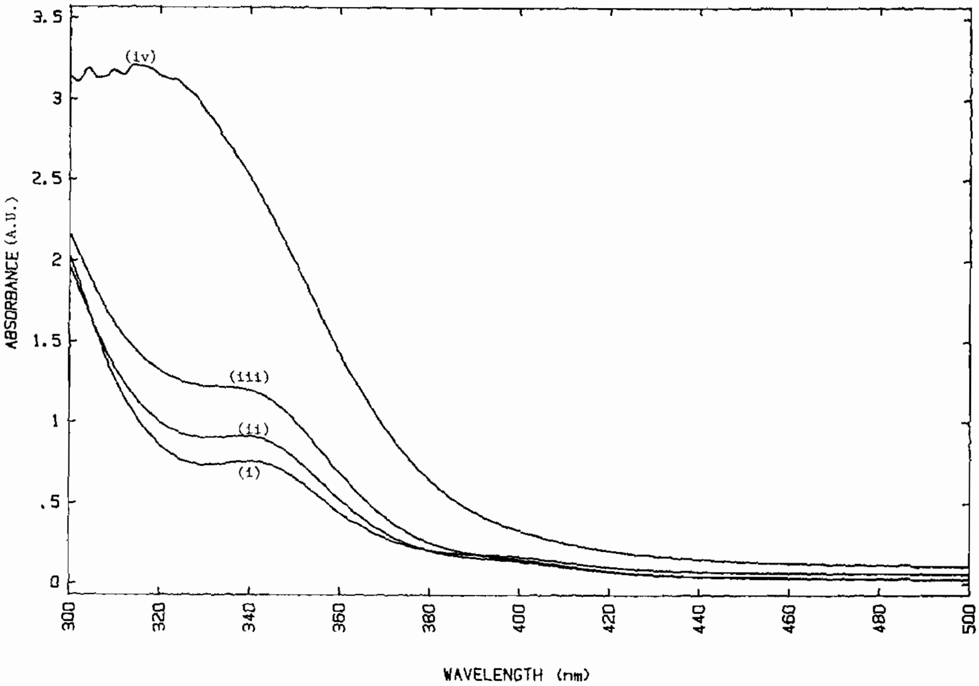

Fig. 5. Changes in absorption spectra of a thin film **1c** on a glass slide during oxidation by gaseous Cl_2: (i) **1c** (0% oxidation); (ii) 11% oxidation; (iii) 27% oxidation; (iv) 100% oxidation. The degree of partial oxidation of the polymer films was determined by the relative absorption intensity at 340 nm.

by a two-probe technique on the Au electrode. No increase in conductivity could be observed in the partially-oxidized or fully-oxidized polymers **1a–c** (Table 2). The results indicate that there is no enhanced intermetallic electronic coupling in the partially-oxidized polymers. The low conductivities of the partially-oxidized polymers **1a–c** are probably caused by the following factors: (i) a decrease of π-backbonding between metal(IV)–phosphine upon the oxidation of the M^{II} centers (M = Ni, Pd, Pt); (ii) a geometry change from square planar (M^{II} centers, M = Ni, Pd, Pt) to tetragonally distorted pseudo-octahedral (M^{IV} centers, M = Ni, Pd, Pt) as the oxidation takes place.

4. Conclusions

The electrochemical and spectroelectrochemical studies of the model bimetallic Ni^{II}, Pd^{II} and Pt^{II} complexes **2a–c** indicate minimal electronic coupling between the two metal centers. The results are consistent with the very low conductivities of the Ni^{II}, Pd^{II} and Pt^{II} phosphine polymers **1a–c**. The low conductivities of the partially-oxidized polymers **1a–c** suggest that charge transfer along the polymer backbone is disrupted by decreased electronic coupling between metal centers and geometric distortion upon oxidation of the metal centers.

Acknowledgement

This work is supported by the Office of Basic Energy Sciences, US Department of Energy.

References

[1] J.R. Reynolds, C.P. Lillya and J.C.W. Chien, *Macromolecules, 20* (1987) 1184.
[2] C.W. Dirk, M. Bousseau, P.H. Barrett, F. Moraes, F. Wudl and A.J. Heeger, *Macromolecules, 19* (1986) 266.
[3] F. Wang and J.R. Reynolds, *Macromolecules, 23* (1990) 3219.
[4] F. Gotzfried, W. Beck, A. Lerf and A. Sebald, *Angew. Chem., Int. Ed. Engl., 18* (1979) 463.
[5] J.T. Wrobleski and D.B. Brown, *Inorg. Chem., 18* (1979) 2738.
[6] O.J. Jacobus and S.B. Owen, *US Patent* No. 4 442 421 (1984); *Chem. Abstr., 101* (1984) 65199v.
[7] T.J. Marks, *Angew. Chem., Int. Ed. Engl., 29* (1990) 857.
[8] M.A. Fox and D.A. Chandler, *NATO ASI Ser. C, 214* (1987) 405.
[9] M.A. Fox and D.A. Chandler, *Adv. Mater., 3* (1991) 381.
[10] P.W. Wang and M.A. Fox, *Inorg. Chem.,* (1994) in press.
[11] A.J. Bard and L.R. Faulkner, *Electrochemical Methods: Fundamentals and Applications,* Wiley, New York, 1980, p. 701.
[12] E.P. Kyba, S.T. Liu and R.L. Harris, *Organometallics, 2* (1983) 1877.
[13] A. Sen and L. Ta-Wang, *J. Am. Chem. Soc., 103* (1981) 4627.
[14] S.D. Ittel, in A.G. MacDiarmid (ed.), *Inorganic Synthesis,* Vol. 17, McGraw-Hill, New York, 1977, p. 117.
[15] S.T. Liu, J.T. Chen, S.M. Peng, Y.L. Hsiao and M.C. Cheng, *Inorg. Chem., 29* (1990) 1169.

[16] L.F. Warren and M.A. Bennett, *Inorg. Chem., 15* (1976) 3126.
[17] C.N. Sethulakshmi, S. Subramainan, M.A. Bennett and P.T. Manoharan, *Inorg. Chem., 18* (1979) 2520.
[18] S.J. Higgins and W. Levason, *J. Chem. Soc., Dalton Trans.,* (1986) 317.
[19] L.R. Gray, D.J. Gulliver, W. Levason and M. Webster, *J. Chem. Soc., Dalton Trans.,* (1983) 133.
[20] A.G. Orpen and N.G. Connelly, *Organometallics, 9* (1990) 1206.
[21] Md.M. Rahman, H.Y. Liu, A. Prock and W.P. Giering, *Organometallics, 6* (1987) 650.
[22] J.E. Huheey, *Inorganic Chemistry: Principles of Structure and Reactivity,* Harper and Row, New York, 1983, p. 368.
[23] M.A. Fox, D.A. Chandler and E.P. Kyba, *J. Coord. Chem., 25* (1992) 1.